

Phase Separation Induced by Polymerization of 2-Chlorostyrene in a Polystyrene/Dibutyl Phthalate Mixture

Mamoru Okada,* Koji Fujimoto, and Takuhei Nose

Department of Polymer Chemistry, Tokyo Institute of Technology,
Ookayama, Meguro-ku, Tokyo 152, Japan

Received October 17, 1994; Revised Manuscript Received December 5, 1994*

ABSTRACT: Phase separation induced by polymerization of 2-chlorostyrene (2ClS) in polystyrene (PS)/di-*n*-butyl phthalate (DBP) mixtures was studied by the time-resolved light scattering (TRLS) technique and scanning electron microscopy. Measurements were performed at a fixed composition of 2ClS:PS:DBP = 45:45:10 by weight in a temperature range from 110 to 180 °C that was above the glass transition temperature of the product. Conversion of 2ClS was estimated by gel permeation chromatography. Two distinct time regions were observed in time dependence of scattered light intensity I_m and conversion of 2ClS. In the first region, I_m and conversion increased rapidly, while in the second region, conversion that had reached about 80% changed very little and the growth rate of I_m became much smaller than that in the first region. The poly(2-chlorostyrene)-rich phase formed droplets, and droplets of relatively narrow distribution coexisted with much smaller droplets in an early period. Nonspherical domains were formed by coalescence of droplets. At lower temperatures, it was observed for the first time that the droplet domain structure transformed into cocontinuous domains. This morphological change occurred while the conversion changed very little. Acceleration of the phase separation rate associated with the morphological change was observed by TRLS. At higher temperatures, coalescence of droplets occurred only in a very early period, and droplets coarsened without forming cocontinuous domains in the later period. The mechanism of the polymerization-induced phase separation of this system is discussed.

Introduction

Phase separation induced by polymerization of components in an initially miscible mixture has been widely investigated in recent years.^{1–12} However, most works have aimed primarily at industrial applications, and the dynamics of polymerization-induced phase separation has not been fully investigated yet. Consequently, little is known about its mechanisms at present, although recent advances in the study¹³ of phase separation of polymer solutions and blends in the absence of reaction are expected to facilitate our understanding of this interesting and important phenomenon. Polymerization-induced phase separation is a highly complicated phenomenon that is enormously difficult to analyze. To avoid unnecessary complications that hinder gaining useful information from experiments, it is desirable to make experimental conditions as simple as possible. Previous works have concentrated on the curing of epoxy resins, reflecting its industrial importance. The curing of epoxy resins is accompanied by network formation (gelation), which brings further complications to the analysis of the experimental results. In addition, network formation pins phase separation, which prohibits investigation of the entire phase separation process.

In this paper, we studied the phase separation process induced by polymerization of a system containing no multifunctional agent by using the time-resolved light scattering (TRLS) technique and scanning electron microscopy. Electron micrographs were taken at various stages of phase separation to follow the morphological changes during phase separation. The sample we used was a mixture of 2-chlorostyrene monomer and polystyrene. The system shows weak segregation after polymerization of the monomer. It is known that poly(2-chlorostyrene) and polystyrene are partially miscible in a certain molecular weight range.^{14–16} All experi-

ments were carried out above the glass transition temperature of the product because vitrification also pins phase separation as gelation does. Since the maximum experimental temperature was limited by sample degradation, we lowered the glass transition temperature by adding a small amount of plasticizer, di-*n*-butyl phthalate, to the sample mixture so that we could extend the experimentally accessible temperature range. Although our interest lies in the entire process of phase separation, we discuss here mainly the later period of phase separation because of the following experimental difficulties encountered in measurements in very early periods. Phase separation was initially very fast and the data acquisition speed of the TRLS instrument we used was not fast enough to follow such a fast process. In addition, since the glass transition temperature of a sample at low conversion of the monomer was low, the electron microscope observation was not possible at room temperature.

Experimental Section

Materials and Sample Preparation. Polystyrene (PS) standards with nominal weight-average molecular weight $M_w = 5.0 \times 10^4$ and polydispersity index $M_w/M_n < 1.06$ were purchased from Pressure Chemical Co. The monomer 2-chlorostyrene (2ClS) was purchased from Tokyo Kasei Kogyo and Aldrich Chemical Co. and purified by distillation from barium oxide under a reduced pressure after the inhibitor was removed by a conventional method. After being purified, the monomer was stored at 5 °C and used within 1 week. The plasticizer, di-*n*-butyl phthalate (DBP, purity >98%) was a product of Tokyo Kasei Kogyo and used without further purification. The sample mixture was prepared by dissolving a desired amount of PS in a mixture of 2ClS and DBP of a known composition followed by stirring overnight to ensure complete mixing. No initiator was added to the mixture, and polymerization was initiated only by increasing the temperature. The sample mixture was placed between two round glass plates with a 0.2 mm thick spacer, and these sample plates were tightly fixed in a holder with a screw. The sample composition was fixed at PS:2ClS:DBP = 45:45:10 by weight in all measurements.

* Abstract published in *Advance ACS Abstracts*, February 1, 1995.

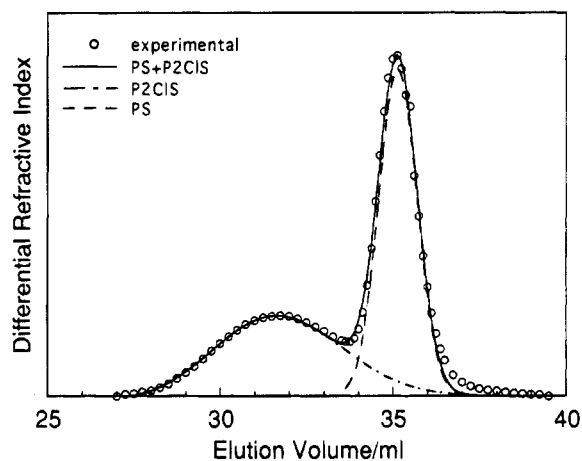


Figure 1. Gel permeation chromatogram of the sample reacted at 140 °C for 6 h. Circles denote experimental results. The P2CIS and PS peaks were separated by the best fit of the Gaussian functions.

Instruments. The time-resolved light scattering measurements were performed with an instrument constructed in this laboratory. A He-Ne laser operated at a wavelength of 632.8 nm was used as a light source, and the transmitted light intensity was monitored by a photodiode. The angular dependence of the scattered light intensity was measured by scanning a photomultiplier tube with a stepping motor. Correction of the scattered light intensity was made for turbidity. The jump from room temperature to a reaction temperature was made by pushing the sample holder manually into a heating block (thermostat) controlled at a desired temperature to ± 0.03 °C. Both the sample holder and the heating block were made of copper, and the temperature of the holder was stabilized within 5 min after the jump.

Microdomain structures during the phase separation were studied by electron microscopy. After a sample cell was kept in the thermostat for a desired period, it was taken out and rapidly quenched to room temperature to fix the morphological structure of the sample. The quench was made by contacting the sample holder with two brass blocks that were cooled to about -15 °C in a refrigerator. Two different kinds of thermostats were used depending on the length of period for which sample was kept in the thermostat: The copper block of the TRLS instrument was used in the case of shorter periods and a thermostat made of an aluminum block that could hold 12 samples simultaneously was used in the case of longer periods. The accuracy of the temperature control of the latter thermostat was the same as that of the former thermostat (i.e., ± 0.03 °C). The backscattered electron image of the microtomed surface was observed with a JEOL JSM-T220 electron microscope operated at 10–15 kV. Good contrast was obtained in electron micrographs without staining.

Conversion of 2-chlorostyrene was estimated by gel permeation chromatography (GPC). The GPC measurements were made by a Toso HLC8 apparatus with a Toso RI-8 differential refractometer as a detector. Figure 1 shows an example of a gel permeation chromatogram of a sample reacted for a certain period. The sharp peak at the larger elution volume corresponds to PS, and the broad peak at the smaller elution volume corresponds to poly(2-chlorostyrene) (P2CIS) produced by polymerization. The amount of P2CIS was determined from the area ratio of these two peaks by correcting for the difference in refractive index increment between the two polymer species in the eluent tetrahydrofuran. As two peaks overlapped with each other, we evaluated the area of each peak by curve fitting. By assuming that the elution curve of the individual polymer species was expressed by a sum of Gaussian functions, we made curve fittings for the elution curves of pure PS and the reacted samples. Fitting results are also shown in Figure 1. When the reaction temperature was raised, the P2CIS peak shifted to a larger elution volume and the overlap with the PS peak became too large to evaluate the respective peak areas precisely. Thus, the conversion of 2CIS was estimated only for samples reacted at lower temperatures.

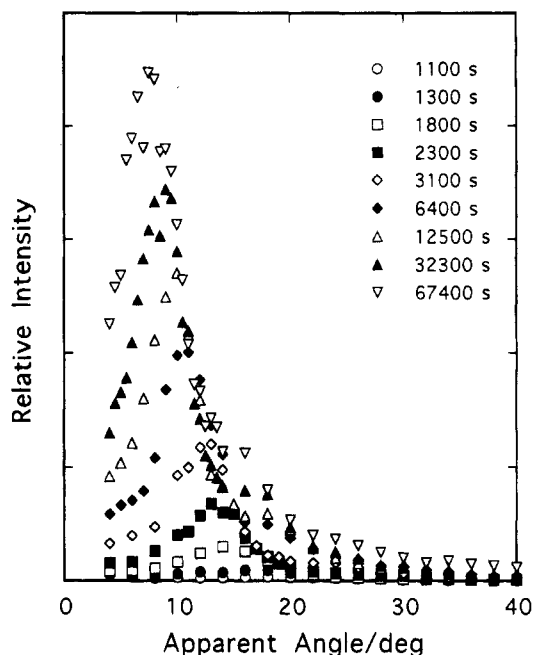


Figure 2. Time evolution of the angular dependence of the light intensity scattered from the sample (2CIS/PS/DBP = 45/45/10) under phase separation induced by polymerization of 2CIS monomer at 160 °C.

Results and Discussion

Time-Resolved Light Scattering. After polymerization was initiated by a temperature jump, the system remained homogeneous until the P2CIS concentration reached the stability limit. The induction time before the scattered intensity started to increase rapidly was largely dependent on temperature, and it decreased from 26.7 min at 110 °C to less than 2 min at 180 °C. Figure 2 shows the time evolution of the scattered intensity profile against the apparent scattering angle for the sample reacted at 160 °C. There was a maximum at a nonzero angle and the maximum point increased in intensity and shifted to smaller angles with time, which was not different from the behavior observed in the ordinary spinodal decomposition in the absence of polymerization. At temperatures other than 160 °C, qualitatively the same behavior was observed.

The maximum intensity I_m and the wavenumber q_m at which the maximum is located are plotted against time for various temperatures in Figure 3, panels a and b, respectively. The variable of the abscissa denotes the phase separation time given by subtracting the induction time t_0 from the time t after the temperature jump. Each set of data is shifted vertically for viewing clarity. Data points of two independent experiments at 160 °C fell on the same curves, which shows good reproducibility of the measurement. Two distinct time regions were observed in the plots of $\log I_m$ versus $\log(t - t_0)$ at all temperatures except 140 °C. In the earlier time region (referred to as region I hereafter, I_m increased quite rapidly but in the succeeding region (region II) the rate of increase of I_m slowed significantly. In region II, I_m could be expressed by a power relation

$$I_m \sim (t - t_0)^\beta \quad (1)$$

The exponent β was largely dependent on temperature as shown in Table 1. The rate of increase of I_m was extremely small in region II at the lowest temperature, 110 °C, although it was still higher than that at the estimated glass transition temperature (about 75 °C).¹⁷

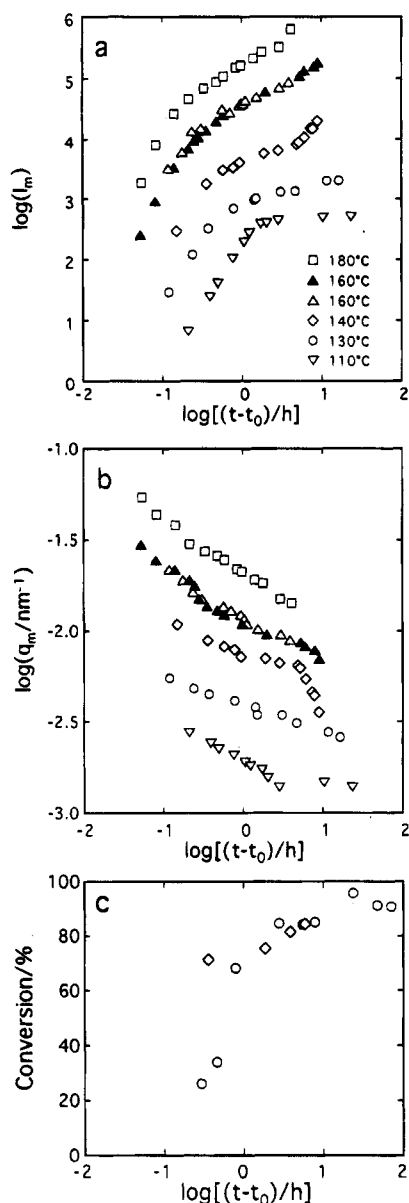


Figure 3. Time dependence of the maximum intensity I_m , wavenumber q_m at which the maximum intensity is located, and conversion of 2ClS at various temperatures. t is the time after the temperature jump and t_0 is the induction time before phase separation occurs. The $\log I_m$ and $\log q_m$ data are vertically shifted by the following amounts 0.5, 0.3 (130 °C); 1.0, 0.6 (140 °C); 1.5, 0.9 (160 °C); 2.0, 1.2 (180 °C).

Table 1. Apparent Values of the Exponents α and β

temp/°C	α		β	
	region II	region III	region II	region III
110	0.05		0.09	
130	0.14		0.34	
140	0.11	1.00	0.42	1.50
160	0.19		0.74	
180	0.27		0.82	

At 140 °C, the rate of increase of I_m was initially rapid, then slowed (which was the same as observed at the other temperatures), but then accelerated again in a later period. Therefore the time dependence of I_m could be divided into three regions rather than two at 140 °C.

Two time regions observed in I_m were not clearly distinguished in q_m as seen in Figure 3b. The wavenumber q_m was fitted to the power relation

$$q_m \sim (t - t_0)^{-\alpha} \quad (2)$$

in the range corresponding to the region II of I_m , and the evaluated exponents α are shown in Table 1. The third time region observed in I_m at 140 °C was clearly distinguished in q_m . The exponent α of region III was evaluated to be 1.0, which was much larger than any exponent of region II, including those at higher temperatures.

Figure 3c shows the conversion of 2ClS at 130 and 140 °C estimated from the gel permeation chromatograms. Polymerization initially proceeded rapidly but its rate became very slow after the conversion reached about 80%. The time dependence of the conversion at 130 °C was quite similar to that of I_m . The phase separation rate depends on the product of mobility and thermodynamic driving force.¹³ An increase in P2ClS concentration results in an increase in the driving force and in a decrease in the mobility, but the contribution of the latter to the phase separation rate is dominant over the contribution of the former except in the vicinity of the stability limit. Therefore it is expected that the phase separation rate will slow down with the conversion of 2ClS, and in fact this agrees with our observation. Although the conversion could not be determined at higher temperatures, it is reasonable to consider that, in region I of I_m , phase separation was rapidly proceeding because the conversion was still low and the mobility was consequently high.

It is noted that the boundary between the regions of distinctive reaction rates was located at a slightly late time compared with the boundary between regions I and II of I_m . That is, there was a period in which the reaction rate was still relatively fast though phase separation had considerably slowed down its rate.

Morphological Structures. Figure 4 shows the domain structures during phase separation at 130 °C observed by the scanning electron microscope. The first three micrographs show the structures in the period covered by the time-resolved light scattering measurements, and the remaining micrographs show the structures at a much later period. The bright parts in the electron micrographs correspond to the P2ClS-rich phase and the dark parts correspond to the PS-rich phase. The P2ClS-rich phase formed droplets in the early period, and these droplets continued to grow with time. At $t = 3$ and 8 h after the temperature jump, it was observed that there were very small droplets among larger droplets of relatively narrow size distribution. This is very different from the droplet structures observed in ordinary phase separations at off-critical compositions.¹⁸ This morphological structure rather resembles the structures observed in droplet deposition and coalescence phenomena such as condensation of a vapor on a surface of a cold substrate.¹⁹ Nonspherical domains formed by coalescence of droplets were observed at $t = 8$ h. The number of such nonspherical domains increased with time. In the later periods, coalescence among more than two droplets occurred and eventually a cocontinuous domain structure similar to those observed in ordinary phase separation at the critical composition was formed as seen in the micrograph at 72 h. This is the first direct observation of the morphological change from droplets to a cocontinuous domain structure, although such morphological change has been proposed to explain the mechanism for formation of the connected-globule structure of epoxy resins.⁵

Although cocontinuous domain structures are known to break into droplets in the late stage of ordinary phase separation in the absence of a polymerization reaction,^{20,21} the morphological change in the opposite

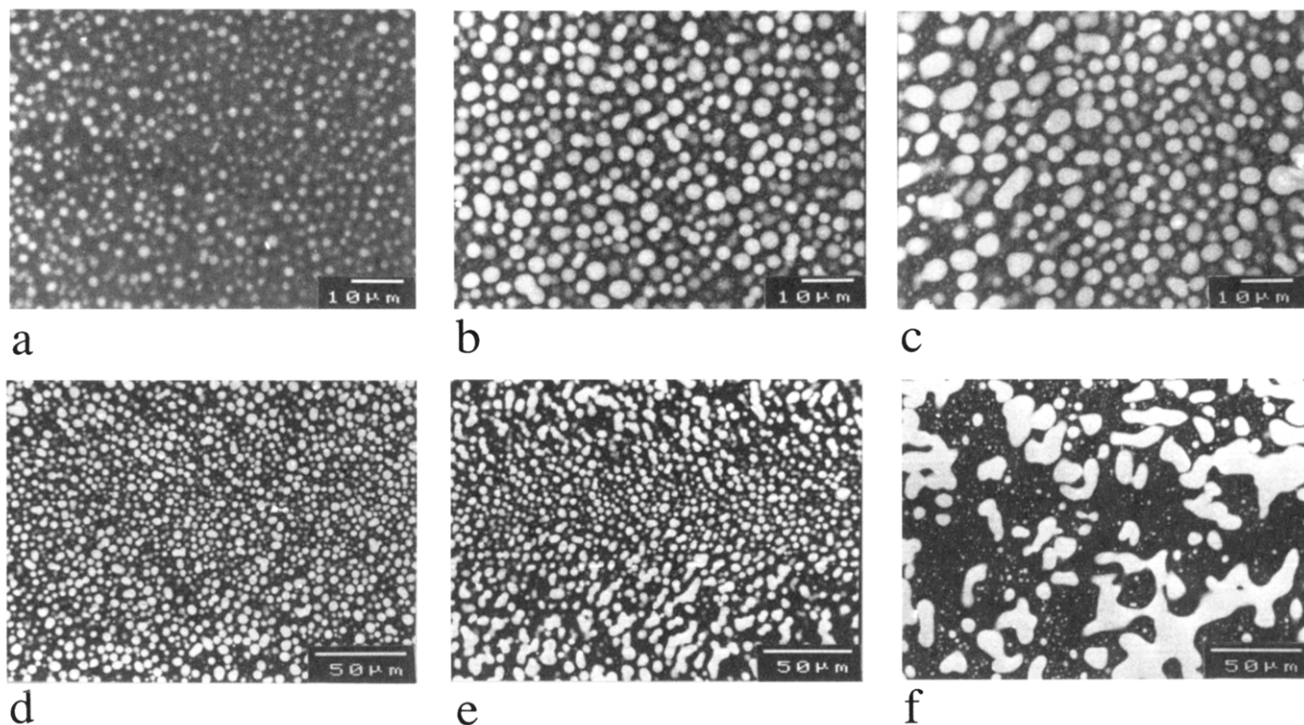


Figure 4. Electron micrographs of a microtomed surface of the sample under phase separation induced by polymerization at 130 °C. Reaction time after temperature jump t = (a) 30 min, (b) 3 h, (c) 8 h, (d) 36 h, (e) 48 h, and (f) 72 h. The bright parts correspond to the P2ClS-rich phase.

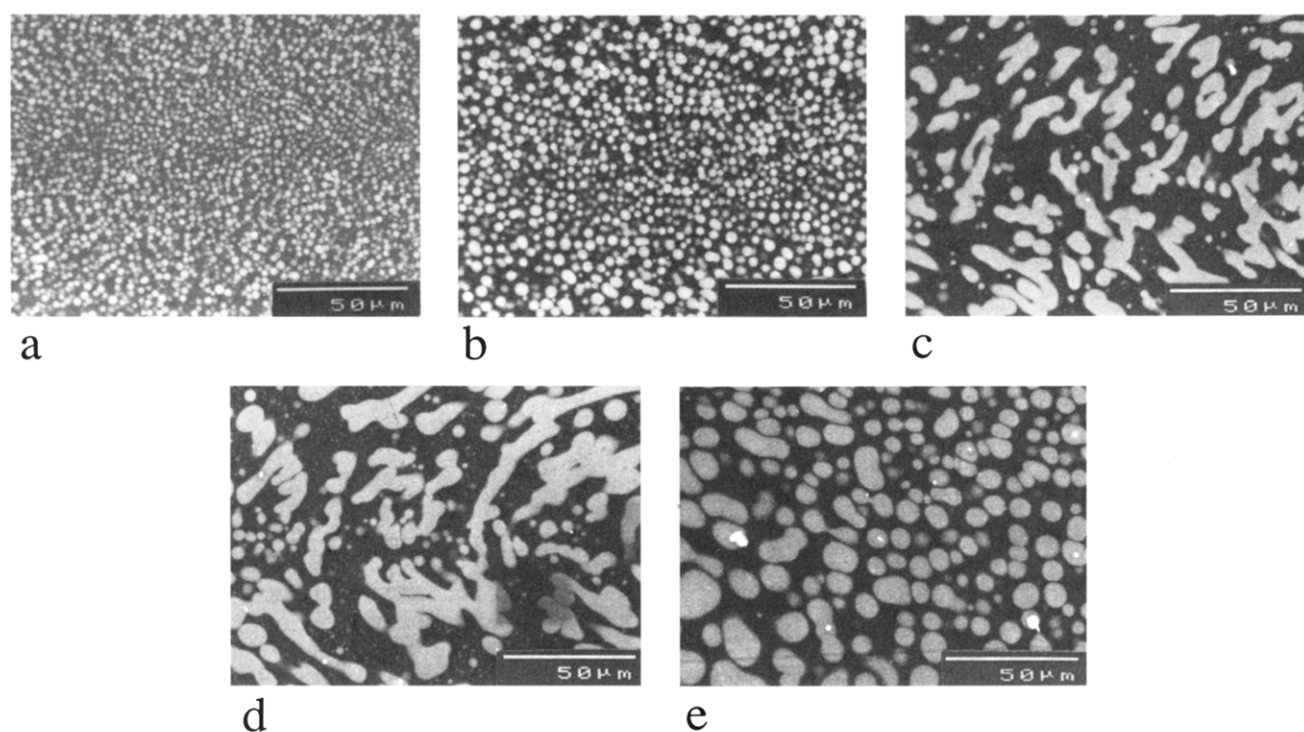


Figure 5. Electron micrographs of a microtomed surface of the sample under phase separation induced by polymerization at 140 °C. Time after temperature jump t = (a) 30 min, (b) 2 h, (c) 4 h, (d) 6 h, and (e) 72 h.

direction, namely the change from droplets to cocontinuous domains, does not take place in ordinary phase separation. In the late stage of ordinary phase separation, the concentration of each phase has attained to the coexisting value, and the total volume of each phase is conserved during the coarsening process. However, in polymerization-induced phase separation, the total volume of each phase is not necessarily conserved, and it is reasonable to consider that the morphological change resulted from the increase in the total volume of droplets. We must notice that the morphological

change occurred while conversion was scarcely increasing. Therefore, it is considered that the P2ClS, which was a major component of the droplet phase, was initially accumulated in the PS-rich background sea domain and was gradually supplied to droplets after polymerization finished.

The phase separation behavior at 140 °C was similar to the behavior at 130 °C as shown in Figure 5. The droplet domain structure emerged initially and grew with time. Nonspherical domains were also observed and grew with time, until the cocontinuous domain

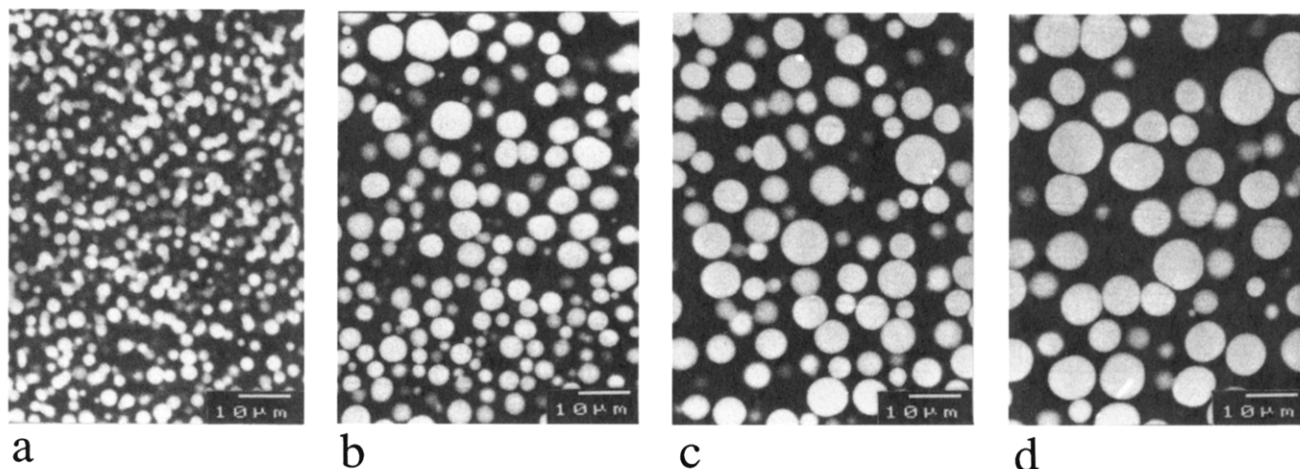


Figure 6. Electron micrographs of a microtomed surface of the sample under phase separation induced by polymerization at 180 °C. Time after temperature jump t = (a) 10 min, (b) 1 h, (c) 6 h, and (d) 24 h.

structure formed. However, in contrast to the case at 130 °C, continuous domains did not extend over the whole system and large regions consisting of only droplets coexisted. The morphological change occurred much earlier than that at 130 °C: It occurred within the period investigated by the time-resolved light scattering experiment. Although the time $t = 4$ h at which cocontinuous domains were already formed was slightly earlier than the beginning of region III observed in the time-resolved light scattering measurement, emergence of region III must be related to formation of the cocontinuous domain structure. In fact, the cocontinuous domain is known to grow much faster than the droplet in fluid systems,²² and this is consistent with acceleration of growth rates of I_m and q_m^{-1} observed in region III. In addition, the exponent $\alpha = 1$ agrees with the theoretical value predicted by Siggia²² for the growth of cocontinuous domains in a fluid system. The time lag between the formation of cocontinuous domains and the beginning of region III suggests that a sharp interface had not yet been formed when cocontinuous domains were formed. It is noted that the cocontinuous domains broke into droplets again at a much later period as seen in Figure 5e. Although the cocontinuous domain structure was not observed at 110 °C, the results at 130 and 140 °C suggest that cocontinuous domains will also be formed at a much longer time than we have investigated.

At higher temperatures, nonspherical domains were formed at an early period but they did not grow large enough to form continuous domains as seen in the case of polymerization at 180 °C shown in Figure 6. Nonspherical domains once formed by coalescence of spherical droplets transformed to spheres in the succeeding period. In the later period, the morphological structures looked very similar to those observed in ordinary phase separation at an off-critical composition. The apparent exponents α and β at 180 °C were not very different from the exponents theoretically predicted for coarsening of spherical domains in ordinary phase separation ($\alpha = 1/3$ and $\beta = 1$).²²

Microdomain Formation Mechanism. We attempted to establish the mechanism of the polymerization-induced phase separation of this system. Here we summarize the experimental results that we must take into consideration for discussing the mechanism. Polymerization initially proceeded very rapidly until conversion became high, and thereafter conversion changed very little. Similarly, the scattered light intensity increased rapidly (after an induction time) and then

reduced its growth rate. The boundary between two time regions in the time-resolved light scattering was located at a slightly earlier time than the boundary in the conversion. The phase rich in the component produced by the polymerization formed droplets, and the distribution of droplet size was very wide in the early period of phase separation: Droplets of relatively narrow size distribution coexisted with much smaller droplets. Nonspherical domains were formed by coalescence of droplets. At lower temperatures, coalescence of droplets occurred frequently, which resulted in transformation of the domain structure to cocontinuous domains. This morphological change occurred while polymerization proceeded very little. Acceleration of the phase separation rate associated with the morphological change occurred after some delay. At higher temperatures, coalescence of droplets occurred only in a very early period and these droplets did not form cocontinuous domains though the phase volume ratio of the droplet phase was not very different from that at lower temperatures.

The plasticizer DBP is a good solvent for PS and P2ClS, and phase separation in the present system is caused by segregation between the two polymer species.¹⁵ In addition, the amount of DBP in the mixture is relatively small. Thus we neglect the plasticizer in the following discussion for simplicity. In that case, the present system is regarded as a ternary system consisting of PS, 2ClS monomer, and its polymerization product, P2ClS. A schematic phase diagram, where the molecular weight distribution is also neglected, is presented in Figure 7. The initial mixture of PS and 2ClS monomer is represented by the midpoint A on the side of the trigonal phase diagram. As polymerization proceeds, the phase point representing the composition of the mixture moves on the line parallel to the side connecting the 2ClS and P2ClS apexes until it reaches the intersection with the phase boundary.

Two extreme cases can be considered regarding the behavior after the phase point moves into the two-phase region, depending on the difference between the phase separation rate and the reaction rate: (i) the polymerization reaction is much faster than phase separation, and (ii) phase separation is fast enough to form domains whose concentrations are very close to the coexisting values at that point. In the former case (i), the phase point continues to move on the same line extended to point B until polymerization finishes somewhere on the line, and very slow phase separation follows. This corresponds to a concentration jump and the phase

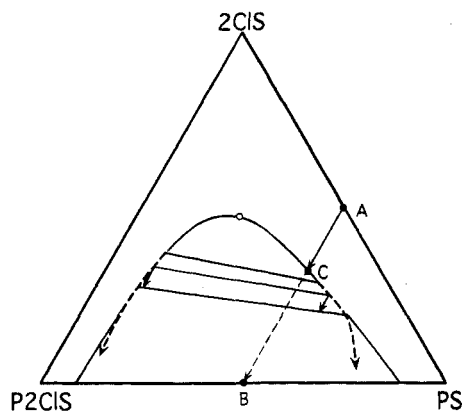


Figure 7. Schematic phase diagram of the ternary system of PS, 2CIS monomer, and the polymerization product P2CIS.

separation behavior is not different from that of the ordinary phase separation induced by a temperature or pressure jump. In the latter case (ii), phase separation proceeds rapidly at shallow points inside the two-phase region, which means that phase separation always occurs at an off-critical composition unless the intersection (point C) is located in the immediate vicinity of the critical point. Droplet domains are formed as a consequence. When the intersection is located on the PS-rich side of the phase diagram, the droplet phase is rich in P2CIS as observed in our experimental results, irrespective of the final phase volume ratio between the two polymers. Polymerization proceeds and P2CIS concentrations in the newly formed domains deviate from the coexisting values. It is noted that, as seen in Figure 7, an increase in the P2CIS concentration in the P2CIS-rich droplet phase results in only a small deviation from the new coexisting concentration compared with the deviation in the PS-rich phase. The excess P2CIS in the background PS-rich phase either diffuses to the existing droplets or causes phase separation leading to the formation of a new generation of droplets, so that the concentration of each phase attains the new coexisting value.

Since phase separation was very fast in the early period as we observed, the phase separation behavior is expected to be very close to the case (ii). As polymerization proceeds, the concentration of P2CIS increases and the system becomes more viscous. The decrease in mobility of the component molecules decreases both phase separation and reaction rates, but the influence on phase separation rate is much larger because long polymer chains have to diffuse for phase separation to proceed while diffusion of small monomer molecules is sufficient for polymerization to proceed. Consequently, as polymerization proceeds, the rate of phase separation is more quickly slowing than the polymerization reaction, and the phase separation behavior becomes more like the case (i). Polymerization finishes in time, and the phase separation behavior strongly depends on how much like the case (i) the phase separation behavior becomes when polymerization finishes. At lower temperatures, since the distance from the glass transition temperature is smaller, the viscosity of the mixture at high conversions is higher than that at higher temperatures. Consequently, with decreasing temperature, the phase separation behavior approaches nearer to the case (i) before polymerization finishes.

When phase separation becomes slow compared with polymerization, the excess P2CIS gradually accumulates in the background domain. After polymerization finishes, phase separation continues to proceed and the total volume of droplets increases, which causes coalescence among droplets. At lower temperatures, a large amount of the excess P2CIS has accumulated and coalescence of droplets leads to formation of a cocontinuous domain structure. On the other hand, at higher temperatures, the amount of excess P2CIS accumulated in the PS-rich phase is insufficient for forming a cocontinuous domain structure, and droplets coarsen without forming cocontinuous domains.

One may consider that morphological change occurred simply because the P2CIS concentration changes from off-critical to critical concentrations as polymerization proceeds, but this does not seem to be consistent with the results at high temperatures. Although the phase volume ratio between the two phases did not deviate very much from unity at high temperatures, cocontinuous structures were not formed. This indicates that formation of a cocontinuous phase is not determined only by the phase volume ratio, and therefore an explanation based on the kinetics of phase separation and polymerization, such as presented here, is necessary.

Acknowledgment. The authors thank Mr. Tsuneo Chiba of the Tokyo Institute of Technology for his help in obtaining the scanning electron micrographs.

References and Notes

- (1) Visconti, S.; Marchessault, R. H. *Macromolecules* **1974**, *7*, 913.
- (2) Manzione, L. T.; Gillham, J. K.; McPherson, C. A. *J. Appl. Polym. Sci.* **1981**, *26*, 889.
- (3) Roginskaya, G. F.; Volkov, V. P.; Bogdanova, L. M.; Chalych, A. Ye.; Rosenberg, B. A. *Polym. Sci. USSR (Engl. Transl.)* **1983**, *25*, 2305.
- (4) Vazquez, A.; Rojas, A. J.; Adabbo, H. E.; Borrajo, J.; Williams, R. J. *J. Polymer* **1987**, *28*, 1156.
- (5) Yamanaka, K.; Inoue, T. *Polymer* **1989**, *30*, 662.
- (6) Yamanaka, K.; Takagi, Y.; Inoue, T. *Polymer* **1989**, *30*, 1839.
- (7) Yamanaka, K.; Inoue, T. *J. Mater. Sci.* **1990**, *25*, 241.
- (8) Moschiar, S. M.; Riccardi, C. C.; Williams, R. J. J.; Verchere, D.; Sautereau, H.; Pascault, J. P. *J. Appl. Polym. Sci.* **1991**, *42*, 717.
- (9) Kim, D. H.; Kim, S. C. *Polym. Eng. Sci.* **1991**, *31*, 289.
- (10) Kim, B. S.; Chiba, T.; Inoue, T. *Polymer* **1993**, *34*, 2809.
- (11) Ruseckaitė, R. A.; Hu, H.; Riccardi, C. C.; Williams, R. J. J. *Polym. Int.* **1993**, *30*, 287.
- (12) Kim, J. Y.; Cho, C. H.; Palfy-Muhoray, P.; Mustafa, M.; Kyu, T. *Phys. Rev. Lett.* **1993**, *71*, 2232.
- (13) For a recent review of phase separation of polymer systems, see: Binder, K. *Adv. Polym. Sci.* **1994**, *112*, 118.
- (14) Alexandrovich, P. S.; Karasz, F. E.; MacKnight, W. J. *J. Macromol. Sci., Phys.* **1980**, *B17*, 501.
- (15) Chu, B.; Linliu, K.; Ying, Q.; Nose, T.; Okada, M. *Phys. Rev. Lett.* **1992**, *68*, 3596.
- (16) Kwak, K. D.; Okada, M.; Chiba, T.; Nose, T. *Macromolecules* **1992**, *25*, 7204.
- (17) Kwak, K. D.; Okada, M.; Nose, T. *Polymer* **1991**, *32*, 864.
- (18) See, for example: Okada, M.; Kwak, K. D.; Chiba, T.; Nose, T. *Macromolecules* **1993**, *26*, 6681.
- (19) Meakin, P. *Rep. Prog. Phys.* **1992**, *55*, 157.
- (20) Hashimoto, T.; Takenaka, M.; Izumitani, T. *J. Chem. Phys.* **1992**, *97*, 679.
- (21) Hasegawa, H.; Shiwa, T.; Nakai, A.; Hashimoto, T. In *Dynamics of Ordering Processes in Condensed Matter*; Komura, S., Furukawa, H., Eds.; Plenum Press: New York, 1988; p 457.
- (22) Siggia, E. D. *Phys. Rev. A* **1979**, *20*, 595.

MA9412795